

Robust Relay Beamforming in Device-to-Device Networks with Energy Harvesting Constraints

Shimin Gong*, Yanyan Shen*, Xiaoxia Huang*, Sissi Xiaoxiao Wu[†], Anthony Man-Cho So[†]

*Shenzhen Institutes of Advanced Technology, Chinese Academy of Sciences, China

[†]Dept. of Systems Engineering and Engineering Management, The Chinese University of Hong Kong, Hong Kong

Abstract—Motivated by the observation that energy harvesting (EH) from radio-frequency (RF) signal is subject to fluctuations, multiple EH-enabled relays are employed to collaboratively enhance data communications in a device-to-device (D2D) network underlying a cellular system. Each relay is equipped with a single antenna and unable to harvest energy and transmit data simultaneously. Thus, the D2D user equipment (DUE) needs to optimally schedule the channel time for the relays' EH and data transmissions, which depends on their EH capabilities and channel conditions. Considering that the relays' channel estimations are usually unreliable, we formulate a robust throughput maximization problem to optimize the relays' EH time and transmit power, subject to a probabilistic interference constraint at the cellular user equipment (CUE). We show that the proposed problem, though non-convex, can be tackled by exploiting its monotonicity structure. Specifically, we design a successive approximation algorithm that involves solving a sequence of semi-definite programs (SDPs) and show numerically that it always achieves the global optimum. This validates our analysis and demonstrates the efficacy of the proposed algorithm.

I. INTRODUCTION

Device-to-device (D2D) communication has recently emerged as a promising technology to support high data rates, extend network coverage, and reduce energy consumptions by enabling direct communications between densely deployed D2D user equipment (DUE) [1]. With the explosive growth of wireless devices, it becomes impractical and costly to recharge or replace batteries for billions of DUEs, especially those deployed in human-inaccessible environment. Wireless power transfer provides a sustainable way to keep connectivity of the D2D networks by allowing the wireless devices to harvest energy from radio frequency (RF) signals [2]. Despite the low cost, RF-based energy harvesting (EH) is still challenging to be widely deployed. Compared to batteries, the energy supply from EH is intermittent in nature and subject to fluctuations due to the dynamics of wireless environment.

Though the amount of energy harvested by single DUE is fluctuating and typically insufficient to sustain wireless transmissions, the dense deployment of DUEs offers a new paradigm for improving network performance. Motivated by the observation that the EH rates (the energy harvested in unit

time duration) are time varying and location dependent, we intend to fully use the harvested energy at different DUEs and improve the throughput performance of a DUE transceiver pair through the DUEs' cooperation. To this end, we are interested in selecting multiple EH-enabled DUE relays to enhance the reliability of information delivery. A single EH relay model has been studied in [3] using either a time switching or power splitting strategy. When multiple relays are available, the authors in [4] proposed a relay selection scheme based on the intuition that each EH relay should be selected with an equal chance to efficiently use the harvested energy. Further analysis in [5] reveals that the optimal selection of EH relays is complicated by the coupling between the channel conditions and the relays' EH capabilities. Considering the limitations of a single relay, some works have studied the collaborative beamforming of multiple EH relays, e.g., [6].

The dense DUE also leads to a crowded usage of the spectrum and may introduce interference to the cellular user equipment (CUE). Hence, the DUE relays need to precisely control their transmit power so that the interference to the CUE is less than a pre-defined threshold. The relays' joint power control under perfect channel information has been studied in [7]. However, in practice, it is very difficult for the DUE relays to collect perfect channel information due to quantization errors and the lack of coordinations between the CUEs and DUEs. Hence, a growing effort has been devoted to modeling the channel uncertainty. A stochastic model assumes that the channel follows a specific Gaussian distribution and leads to a chance-constrained beamforming problem [8], while the worst-case robust model restricts the channel to be bounded in a convex set and leads to a max-min beamforming problem [9]. A more practical way is to build the channel models based on partial distribution information such as the moment statistics that are relatively easy to estimate with high accuracy.

In this paper, by leveraging on the cooperation gain of the densely deployed DUEs, we employ multiple EH-enabled DUE relays operating in a half-duplex mode to enhance the DUEs' data transmissions. On one hand, the relays' transmit powers are subject to *floating* power budget constraints that depend on their EH rates and the time duration for EH. On the other hand, the relays' power control task is complicated by the imperfect channel information and aggregate interference constraints at the CUEs. To the best of our knowledge, we are the first to consider both aspects and jointly design the

This work was supported in part by the National Natural Science Foundation of China under Grant No. 61503368, 61601449, U1501255, and U1301256; the Guangdong Science and Technology Project under Grant No. 2015A010103009; the Shenzhen Science and Technology Project under Grant No. CXZZ20150401152251212, JCYJ20150401150223648, and JCYJ20150401145529016.

relays' EH scheduling and beamforming strategies that are *globally optimal* in the throughput and *resilient* to the channel uncertainty.

The rest of this paper is organized as follows. We describe the system model in Section II and present the relays' joint EH scheduling and beamforming in Section III. Evaluations and conclusions are given in Sections IV and V, respectively.

II. SYSTEM MODEL

We consider a D2D network underlying a downlink cellular system, wherein each DUE transmitter (DTx), DUE relay, and DUE receiver (DRx) have single antenna. The CUE's information reception is not interrupted if the interference due to D2D communications is less than a pre-defined threshold. To fully utilize the harvested energy and improve the DUE's data rate, the DTx is assisted by a group of nearby DUE relays, denoted as $\mathcal{N} = \{1, 2, \dots, N\}$. A direct link between the DTx and DRx is not available due to a long distance or limited transmit power at the DTx. We assume that there is a coordinator in the system that schedules D2D transmissions to avoid conflicts between different DUEs [10].

A. Channel Uncertainty

Let h_n and g_n denote the channels from the DTx to DUE relay n and from the relay n to the DRx, respectively, and z_n denote the channel from the relay n to the CUE. All channels exhibit frequency non-selective block fading. We assume that the channel $\mathbf{h} \triangleq [h_1, h_2, \dots, h_N]^T$ in the first hop is perfectly known through the relays' channel estimation—e.g., the DTx can broadcast a known pilot signal to facilitate the channel estimation. However, due to limited or untimely responses from the DRx and the CUE, the DUE relays are unable to accurately estimate the channels $\mathbf{g} \triangleq [g_1, g_2, \dots, g_N]^T$ and $\mathbf{z} \triangleq [z_1, z_2, \dots, z_N]^T$ in the second hop.

To model the uncertainties of \mathbf{g} and \mathbf{z} , we assume that \mathbf{g} and \mathbf{z} are random variables following distributions $\mathbb{P}_{\mathbf{g}}$ and $\mathbb{P}_{\mathbf{z}}$, respectively. However, the exact probability density functions are not known for sure and are drawn from a set of distribution functions, also known as a distributional uncertainty set [11]. Since it is relatively easy to estimate the moment statistics, we assume that

$$\mathbb{P}_{\mathbf{g}} \in \mathcal{P}(\mathbf{u}_{\mathbf{g}}, \mathbf{S}_{\mathbf{g}}) \subset \mathcal{P}_{\infty}, \quad (1a)$$

$$\mathbb{P}_{\mathbf{z}} \in \mathcal{P}(\mathbf{u}_{\mathbf{z}}, \mathbf{S}_{\mathbf{z}}) \subset \mathcal{P}_{\infty}, \quad (1b)$$

where $\mathcal{P}(\mathbf{u}_{\mathbf{g}}, \mathbf{S}_{\mathbf{g}})$ and $\mathcal{P}(\mathbf{u}_{\mathbf{z}}, \mathbf{S}_{\mathbf{z}})$ denote the sets of distributions with known first- and second-order moments given by $(\mathbf{u}_{\mathbf{g}}, \mathbf{S}_{\mathbf{g}})$ and $(\mathbf{u}_{\mathbf{z}}, \mathbf{S}_{\mathbf{z}})$, respectively, and \mathcal{P}_{∞} is the set of all probability distributions.

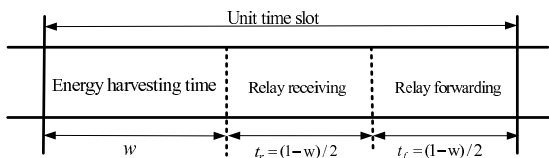


Fig. 1: Time slotted structure.

B. EH Scheduling

We assume that each DUE relay is capable of harvesting energy from the RF signals. To avoid conflicts between EH and information transmissions, we consider the time splitting scheme shown in Fig. 1. Each time slot is of unit length and allocated to relay-assisted transmission of data packets. The first part of a time slot $w \in [0, 1]$ is used for the DUE relays to harvest RF energy and store it in a super-capacitor [2]. The remaining part $1 - w$, without loss of generality, is equally allocated for signal reception and forwarding; i.e., the channel time for signal forwarding is given by $t = (1-w)/2 \in [0, 1/2]$. To gain optimal throughput, the DUE transmitter can adjust the time length for EH and data transmissions according to its channel conditions and energy status. Let $\mathbf{c} \triangleq [c_1, c_2, \dots, c_N]$ denote the vector of EH rates at the DUE relays. We assume that it is known at the beginning of each time slot, as the strength of RF signals changes in a much larger time scale than the time slot for data transmissions [6].

C. Relay Beamforming

We consider the amplify-and-forward (AF) relay strategy due to its short processing delay and simplicity in system deployment. Given the EH time w , the peak transmit power of the relay n is given by $p_n = c_n w / t = c_n (1/t - 2)$. However, relays do not necessarily transmit at their peak power to suppress the noise received by DRx. Let $x_n \in [0, 1]$ denote a power scaling factor such that the actual transmit power is $x_n^2 p_n$, and we view $\mathbf{x} = [x_1, x_2, \dots, x_N]^T$ as the relays' beamformer. Then, the interference at the CUE is given by

$$\phi(t, \mathbf{x}) = \sum_{n=1}^N z_n^2 x_n^2 p_n = \sum_{n=1}^N z_n^2 x_n^2 c_n (1/t - 2). \quad (2)$$

Let s denote the signal transmitted from DTx to the relays, and thus the received signal at relay n is given by $m_n = \sqrt{p_0} h_n s + \sigma_n$, where $\sigma_n \sim \mathbf{N}(0, 1)$ is the Gaussian noise with zero mean and unit variance. The downlink transmissions from the cellular base station to CUEs also introduce interference to the DRx. Here, we assume that such interference is constant and thus omitted in the problem formulation. Assuming unit transmit power at the DTx, the signal strength of m_n is given by $1 + p_0 h_n^2$; i.e., the DUE relay n amplifies the received signal m_n by the coefficient $\bar{x}_n \triangleq x_n \left(\frac{p_n}{1 + p_0 h_n^2} \right)^{1/2}$. Therefore, the received signal at the DRx is given by

$$y = \sum_{n=1}^N \sqrt{p_0} \bar{x}_n h_n g_n s + \sum_{n=1}^N \bar{x}_n g_n \sigma_n + v_d, \quad (3)$$

where $v_d \sim \mathbf{N}(0, 1)$ is the noise in reception. The first term in (3) contains the information from the DTx, while the second term is the amplified noise. The signal-to-noise ratio (SNR) at the DRx is thus represented as follows:

$$\gamma(t, \mathbf{x}) = p_0 \left(\sum_{n=1}^N \bar{x}_n g_n h_n \right)^2 / \left(1 + \sum_{n=1}^N \bar{x}_n^2 g_n^2 \right). \quad (4)$$

Without loss of generality, we can set $p_0 = 1$ for simplicity. Our target is to maximize the DUE's effective throughput in a time slot $r(t, \mathbf{x}) = t \log(1 + \gamma(t, \mathbf{x}))$ by choosing the DUE relays' EH time $w = 1 - 2t$ and the beamformer \mathbf{x} , subject to the CUE's interference constraint $\phi(t, \mathbf{x}) \leq \bar{\phi}$, where $\bar{\phi}$ represents the CUE's tolerance to interference.

III. ROBUST EH SCHEDULING AND BEAMFORMING

Both the throughput $r(t, \mathbf{x})$ and the aggregate interference $\phi(t, \mathbf{x})$ are functions of the channel conditions. Thus, they become stochastic when the channels \mathbf{g} and \mathbf{z} are subject to uncertainties. In the case, we consider maximizing an averaged performance and define the CUE's interference constraint in a probabilistic manner. To facilitate our discussion, we define two constant matrices as follows:

$$\mathbf{H} = \mathbf{D} \left(\mathbf{h} \circ \left[\frac{\sqrt{c_1}}{\sqrt{1+h_1^2}}, \frac{\sqrt{c_2}}{\sqrt{1+h_2^2}}, \dots, \frac{\sqrt{c_N}}{\sqrt{1+h_N^2}} \right]^T \right),$$

$$\mathbf{T} = \mathbf{D} \left(\mathbf{c} \circ \left[\frac{1}{1+h_1^2}, \frac{1}{1+h_2^2}, \dots, \frac{1}{1+h_N^2} \right]^T \right),$$

where “ \circ ” represents the Hadamard product and $\mathbf{D}(\cdot)$ denotes a diagonal matrix with the given diagonal elements.

Considering the uncertainty of channel \mathbf{g} , we rewrite the average SNR at the DRx as follows:

$$\gamma(t, \mathbf{x}) = \frac{\mathbb{E}_{\mathbb{P}_{\mathbf{g}}}[\mathbf{x}^T \mathbf{H} \mathbf{g} \mathbf{g}^T \mathbf{H} \mathbf{x}]}{f(t) + \mathbb{E}_{\mathbb{P}_{\mathbf{g}}}[\mathbf{x}^T \mathbf{T} \mathbf{D}(\mathbf{g} \circ \mathbf{g}) \mathbf{x}]} = \frac{\mathbf{x}^T \mathbf{H} \mathbf{S}_{\mathbf{g}} \mathbf{H} \mathbf{x}}{f(t) + \mathbf{x}^T \mathbf{T} \mathbf{D}(\mathbf{u}_{\mathbf{g}}^s) \mathbf{x}},$$

where $f(t) = t/(1 - 2t) = t/w$ and $\mathbf{u}_{\mathbf{g}}^s = \mathbb{E}_{\mathbb{P}_{\mathbf{g}}}[\mathbf{g} \circ \mathbf{g}]$ is known by the DUE relays. To account for the uncertainty of the channel \mathbf{z} , we define a probabilistic interference constraint for the CUE and thus reformulate the robust EH scheduling and beamforming problem as follows:

$$\max_{t, \mathbf{x}} t \log \left(1 + \frac{\mathbf{x}^T \mathbf{H} \mathbf{S}_{\mathbf{g}} \mathbf{H} \mathbf{x}}{f(t) + \mathbf{x}^T \mathbf{T} \mathbf{D}(\mathbf{u}_{\mathbf{g}}^s) \mathbf{x}} \right) \quad (5a)$$

$$\text{s.t.} \quad \max_{\mathbb{P}_{\mathbf{z}} \in \mathcal{P}(\mathbf{u}_{\mathbf{z}}, \mathbf{S}_{\mathbf{z}})} \mathbb{P}_{\mathbf{z}}(\phi(t, \mathbf{x}) \geq \bar{\phi}) \leq \eta, \quad (5b)$$

$$t \in [0, 1/2] \quad \text{and} \quad \mathbf{x} \in [0, 1]. \quad (5c)$$

Here, we jointly optimize (t, \mathbf{x}) to achieve the optimal throughput for the DUE transceiver pair while limiting the CUE's worst-case (with respect to all distributions with the given moment information) interference violation probability below a prescribed probability limit η . Note that we only consider one CUE in problem (5). However, it can be extended to the case with multiple CUEs, which allows us to protect the most vulnerable CUE. The probabilistic constraint (5b) is generally non-convex and its tractability largely depends on its convex approximation. Besides, the objective (5a) defines a complicated non-concave function of (t, \mathbf{x}) . Nevertheless, by a change of variable, we can view γ as the variable to be optimized instead of \mathbf{x} . Hence, we can represent $r(t, \mathbf{x})$ in a simpler form; i.e., $r(t, \gamma) = t \log(1 + \gamma)$. In the sequel, we use $r(t, \gamma)$ and $r(t, \mathbf{x})$ interchangeably to denote the objective function in (5a). Note that $r(t, \gamma)$ is increasing in t and γ ,

which implies that the global optimum is achieved on the boundary of the feasible region of (t, γ) . This observation motivates us to design an iterative search algorithm by exploiting the monotonicity of the objective function and the structure of the feasible region of (t, γ) .

A. Elements of Monotonic Optimization

The theory of monotonic optimization is developed by Tuy [12] and has been applied to wireless communications [13]. Here, we review some of the basic concepts.

Definition 1 (Boxes): Let $\mathbf{a} \preceq \mathbf{1} \mathbf{b}$. Then, the box $[\mathbf{a}, \mathbf{b}]$ is the set of all $\mathbf{z} \in \mathcal{R}^n$ satisfying $\mathbf{a} \preceq \mathbf{z} \preceq \mathbf{b}$.

Definition 2 (Polyblocks): A polyblock \mathcal{P} is a union of finite number of boxes; i.e., $\mathcal{P} = \bigcup_{\mathbf{v} \in V} [\mathbf{0}, \mathbf{v}]$, where V is the vertex set of the polyblock and $|V| < +\infty$.

Definition 3 (Normal sets): A set Ω is normal if for any $\mathbf{z} \in \Omega$, all other points \mathbf{z}' such that $0 \preceq \mathbf{z}' \preceq \mathbf{z}$ are also in Ω . A point $\mathbf{z} \in \Omega$ is an upper boundary point if $\mathbf{z}' \notin \Omega$ for any $\mathbf{z}' \succeq \mathbf{z}$ and $\mathbf{z}' \neq \mathbf{z}$. The set of upper boundary points of Ω is denoted by $\partial^+ \Omega$.

Proposition 1 (Monotonic optimization): The optimum of an increasing function over a compact normal set Ω is attained on the upper boundary $\partial^+ \Omega$.

Proposition 1 is rather intuitive and a formal proof easily follows from the results in [12]. To reformulate (5) into a monotonic optimization problem, we need to check whether the feasible set of (t, γ) is normal. To this end, we rewrite the feasible set of (t, γ) as follows:

$$\Omega = \left\{ (t, \gamma) \left| \begin{array}{l} \max_{\mathbb{P}_{\mathbf{z}}} \mathbb{P}_{\mathbf{z}}(\phi(t, \mathbf{x}) \geq \bar{\phi}) \leq \eta, \\ 0 \leq \gamma \leq \bar{\gamma} \triangleq \frac{\mathbf{x}^T \mathbf{A} \mathbf{x}}{f(t) + \mathbf{x}^T \mathbf{B} \mathbf{x}}, \\ (t, \mathbf{x}) \in \Theta \triangleq [0, \frac{1}{2}] \times [0, 1] \end{array} \right. \right\}, \quad (6)$$

where $\mathbf{A} = \mathbf{H} \mathbf{S}_{\mathbf{g}} \mathbf{H}$ and $\mathbf{B} = \mathbf{T} \mathbf{D}(\mathbf{u}_{\mathbf{g}}^s)$ are two known matrices relating to the DUE relays' EH rates and channel conditions. Now, we can simply reformulate problem (5) as follows:

$$\max_{t, \gamma} \{r(t, \gamma) : (t, \gamma) \in \Omega\}. \quad (7)$$

Proposition 2: The feasible set Ω is normal.

The proof of Proposition 2 is given in Appendix A. The basic idea of monotonic optimization is to successively approximate the feasible set Ω by polyblocks. The initial polyblock P_0 can be large enough to cover the whole feasible set Ω , and thus we can set the vertex of P_0 to be $(1/2, \gamma_{max})$, where γ_{max} denotes the largest possible γ for $t \in [0, 1/2]$ and $\mathbf{x} \in [0, 1]$. Note that $\gamma < \frac{\mathbf{x}^T \mathbf{A} \mathbf{x}}{\mathbf{x}^T \mathbf{B} \mathbf{x}}$ and the maximum of $\frac{\mathbf{x}^T \mathbf{A} \mathbf{x}}{\mathbf{x}^T \mathbf{B} \mathbf{x}}$ is confined by the largest eigenvalue of $\mathbf{B}^{-1} \mathbf{A}$ [14], which relates to the relays' EH rates and channel conditions.

In the k -th iteration, the algorithm first determines an upper bound r_k^U of the global optimum—i.e., $r_k^U = \max_{\mathbf{z} \in P_k} r(\mathbf{z})$ —which will be achieved by one of the vertices of P_k due to

¹ $\mathbf{a} \preceq \mathbf{b}$ (or $\mathbf{a} \succeq \mathbf{b}$) means that $\mathbf{b} - \mathbf{a}$ (or $\mathbf{a} - \mathbf{b}$) has non-negative entries.

the monotonicity of the objective. Then, it updates a lower bound r_k^L by evaluating the objective at one feasible point o_k on the upper boundary. Moreover, the point o_k allows us to trim P_k and generate a “smaller” polyblock, which results in $P_{k+1} \subset P_k$. The algorithm continues until the gap between the upper and lower bounds is within an error distance limit ϵ .

B. Lower Throughput Bounds via Projection

Given the polyblock P_k , the upper throughput bound can be easily obtained from one of the vertices of P_k . Let $\mathbf{z}_k = \arg \max_{\mathbf{v} \in V_k} r(\mathbf{v})$, where V_k denotes the vertex set of P_k . Then, $r_k^U = r(\mathbf{z}_k)$ can serve as an upper bound on the optimum $r^* = \max_{\mathbf{z} \in \Omega} r(\mathbf{z})$ due to the monotonicity of the objective function. To find a lower bound on r^* , we project the vertex \mathbf{z}_k onto $\partial^+ \Omega$ by scaling it down, as illustrated in Fig. 2a. Define $\mathbf{o}_k(s) = s\mathbf{z}_k$ as the scaled vertex \mathbf{z}_k .

The projection requires finding the maximum scaling factor s_k to ensure $\mathbf{o}_k(s_k) \in \Omega$. Noting that Ω is normal, we have $\mathbf{o}_k(s) \notin \Omega$ for $s \in (s_k, 1]$ and $\mathbf{o}_k(s) \in \Omega$ for $s \in [0, s_k]$, which suggests a bisection method to pinpoint s_k . Given a fixed scaling factor s in the k -th iteration, checking whether $\mathbf{o}_k(s) \in \Omega$ is equivalent to finding some $\mathbf{x} \in [0, 1]$ such that

$$\frac{\mathbf{x}^T \mathbf{A} \mathbf{x}}{f(st_k) + \mathbf{x}^T \mathbf{B} \mathbf{x}} \geq s\gamma_k, \quad (8a)$$

$$\max_{\mathbb{P}_{\mathbf{z}} \in \mathcal{P}(\mathbf{u}_{\mathbf{z}}, \mathbf{S}_{\mathbf{z}})} \mathbb{P}_{\mathbf{z}}(\phi(st_k, \mathbf{x}) \geq \bar{\phi}) \leq \eta. \quad (8b)$$

Note that (8a) implies $s\gamma_k f(st_k) \leq \mathbf{x}^T (\mathbf{A} - s\gamma_k \mathbf{B}) \mathbf{x}$. Hence, the feasibility check can be performed in two steps. First, we maximize $\mathbf{x}^T (\mathbf{A} - s\gamma_k \mathbf{B}) \mathbf{x}$ subject to (8b); i.e.,

$$p(s, \mathbf{z}_k) \triangleq \max_{\mathbf{x} \in [0, 1]} \mathbf{x}^T (\mathbf{A} - s\gamma_k \mathbf{B}) \mathbf{x} \quad (9a)$$

$$s.t. \quad \max_{\mathbb{P}_{\mathbf{z}} \in \mathcal{P}(\mathbf{u}_{\mathbf{z}}, \mathbf{S}_{\mathbf{z}})} \mathbb{P}_{\mathbf{z}}(\phi(st_k, \mathbf{x}) \geq \bar{\phi}) \leq \eta. \quad (9b)$$

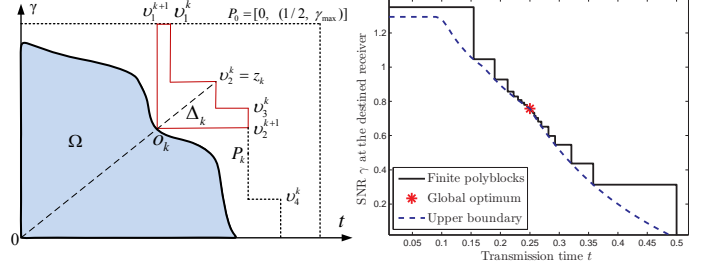
Then, we compare the maximum $p(s, \mathbf{z}_k)$ to $s\gamma_k f(st_k)$. If $p(s, \mathbf{z}_k) \geq s\gamma_k f(st_k)$, then $\mathbf{o}_k(s) \in \Omega$ and we can increase the scaling factor s in the next iteration. The availability of $p(s, \mathbf{z}_k)$ is essential to finding the accurate scaling factor s_k and ensuring the convergence of the polyblock approximation algorithm. However, it is not straightforward to find a solution to problem (9) due to the possibly indefinite matrix coefficient $(\mathbf{A} - s\gamma_k \mathbf{B})$ in (9a) and the probabilistic constraint in (9b).

In the sequel, we first derive a convex equivalence for (9b) and then propose a semi-definite relaxation (SDR) to transform the quadratic objective (9a) into a linear trace form. Note that

$$\phi(st_k, \mathbf{x}) = \sum_{n=1}^N z_n^2 x_n^2 c_n \left(\frac{1}{st_k} - 2 \right) = \mathbf{z}^T \mathbf{D}(\mathbf{x} \circ \mathbf{x}) \mathbf{D}(\mathbf{c}_s) \mathbf{z},$$

where $\mathbf{c}_s = \left(\frac{1}{st_k} - 2 \right) \mathbf{c}$ denotes the scaled EH rates at the DUE relays. Let $e(\mathbf{z}) = \mathbf{1}(\mathbf{z}^T \mathbf{D}(\mathbf{x} \circ \mathbf{x}) \mathbf{D}(\mathbf{c}_s) \mathbf{z} \geq \bar{\phi})$, where $\mathbf{1}(\cdot)$ is the indicator function. For a fixed (st_k, \mathbf{x}) , we define

$$B(st_k, \mathbf{x} | \Sigma_{\mathbf{z}}) = \max_{\mathbb{P}_{\mathbf{z}} \in \mathcal{P}(\mathbf{u}_{\mathbf{z}}, \mathbf{S}_{\mathbf{z}})} \mathbb{E}_{\mathbb{P}_{\mathbf{z}}} [e(\mathbf{z})]$$



(a) Polyblock approximation

(b) An illustrative example

Fig. 2: Successive polyblock approximations.

as the worst-case interference violation probability on the LHS of (9b), where $\Sigma_{\mathbf{z}} = \begin{bmatrix} \mathbf{S}_{\mathbf{z}} & \mathbf{u}_{\mathbf{z}} \\ \mathbf{u}_{\mathbf{z}}^T & 1 \end{bmatrix}$ denotes the second order moment matrix of the channel \mathbf{z} . We can easily find that $B(st_k, \mathbf{x} | \Sigma_{\mathbf{z}})$ admits an equivalent form as follows [15]:

$$\min_{\mathbf{M} \succeq 0, \nu \geq 0} \text{Tr}(\Sigma_{\mathbf{z}} \mathbf{M}) \quad (10a)$$

$$s.t. \quad \mathbf{M} \succeq \begin{bmatrix} \nu \mathbf{D}(\mathbf{x} \circ \mathbf{x}) \mathbf{D}(\mathbf{c}_s) & 0 \\ 0 & 1 - \nu \bar{\phi} \end{bmatrix}, \quad (10b)$$

where \mathbf{M}, ν are the dual variables. To this point, the objective (10a) is linear and the constraint (10b) is a linear matrix inequality. Hence, problem (10) provides a convex equivalence for $B(st_k, \mathbf{x} | \Sigma_{\mathbf{z}})$. Substituting (10) into (9b), the beamformer \mathbf{x} can be optimally obtained as follows:

$$p(s, \mathbf{z}_k) \triangleq \max_{\mathbf{x}, \mathbf{M}, \nu} \mathbf{x}^T (\mathbf{A} - s\gamma_k \mathbf{B}) \mathbf{x} \quad (11a)$$

$$s.t. \quad \text{Tr}(\Sigma_{\mathbf{z}} \mathbf{M}) \leq \nu \eta, \quad (11b)$$

$$\mathbf{M} \succeq \begin{bmatrix} \mathbf{D}(\mathbf{x} \circ \mathbf{x}) \mathbf{D}(\mathbf{c}_s) & 0 \\ 0 & \nu - \bar{\phi} \end{bmatrix}, \quad (11c)$$

$$\mathbf{M} \succeq 0, \quad \nu \geq 0, \quad \mathbf{0} \leq \mathbf{x} \leq \mathbf{1}. \quad (11d)$$

However, problem (11) is still non-convex with respect to \mathbf{x} due to the quadratic terms of \mathbf{x} in (11a) and (11c). To circumvent this difficulty, we introduce a rank-one matrix $\mathbf{X} = \mathbf{x} \mathbf{x}^T$. Thus, we have $\mathbf{x}^T (\mathbf{A} - s\gamma_k \mathbf{B}) \mathbf{x} = \text{Tr}(\mathbf{X} (\mathbf{A} - s\gamma_k \mathbf{B}))$ and $\mathbf{D}(\mathbf{x} \circ \mathbf{x}) = \Delta(\mathbf{X})$, where $\Delta(\mathbf{X})$ is the diagonal matrix by setting all off-diagonal elements to zeros. As an approximation, we drop the non-convex rank-one constraint on \mathbf{X} and obtain the SDR representation of problem (11):

$$p(s, \mathbf{z}_k) \triangleq \max_{\mathbf{X}, \mathbf{M}, \nu} \text{Tr}(\mathbf{X} (\mathbf{A} - s\gamma_k \mathbf{B})) \quad (12a)$$

$$s.t. \quad \text{Tr}(\Sigma_{\mathbf{z}} \mathbf{M}) \leq \nu \eta, \quad (12b)$$

$$\mathbf{M} \succeq \begin{bmatrix} \Delta(\mathbf{X}) \mathbf{D}(\mathbf{c}_s) & 0 \\ 0 & \nu - \bar{\phi} \end{bmatrix}, \quad (12c)$$

$$\mathbf{M} \succeq 0, \quad \nu \geq 0, \quad \mathbf{0} \leq \mathbf{X} \leq \mathbf{I}. \quad (12d)$$

Note that (12a) and (12b) are linear and (12c) defines a linear matrix inequality. Thus, problem (12) is an semi-definite program (SDP) that can be efficiently solved by interior-point algorithms. If the optimal \mathbf{X}^* happens to be rank one, a feasible solution \mathbf{x}^* to (9) can be extracted by eigen-decomposition. Otherwise, we extract from \mathbf{X}^* an approximate

rank-one solution by a Gaussian randomization method [16]. While it is still an open question to formally prove the existence of a rank-one solution in (12), extensive numerical experiments in this work show that \mathbf{X}^* is always rank-one and a similar observation has been mentioned in [11].

C. Generation of New Polyblock

If the vertex \mathbf{z}_k happens to be on the upper boundary, then we have $r_k^U = r_k^L$ and thus \mathbf{z}_k is the optimal solution. If $\mathbf{z}_k \neq \mathbf{o}_k$, then r_k^U is unattainable and we need to shrink the polyblock in the next iteration. Specifically, we construct a separating cone $P_k^c \triangleq \{\mathbf{z} \mid \mathbf{z} \succeq \mathbf{o}_k\}$ such that $P_k^c \cap \Omega = \emptyset$. As illustrated in Fig. 2a, we can generate a new polyblock P_{k+1} by cutting off $\Delta_k \triangleq P_k^c \cap P_k = \{\mathbf{z} \in P_k \mid \mathbf{z} \succeq \mathbf{o}_k\}$ from the polyblock P_k and it is easy to verify that

$$\Omega \subset P_{k+1} \triangleq P_k \setminus \Delta_k \subset P_k.$$

Moreover, the removal of Δ_k will remove some vertices in V_k but also generate some new ones. Let $\bar{V}_k(\mathbf{o}_k) = \{\mathbf{v} \in V_k \mid \mathbf{v} \succeq \mathbf{o}_k\}$ denote the set of vertices that are removed from V_k and define $\bar{\mathbf{z}}_k(i) = \max_{\mathbf{v} \in \bar{V}_k(\mathbf{o}_k)} \mathbf{v}(i)$ for $i \in \{1, 2\}$, where $\mathbf{v}(i)$ and $\bar{\mathbf{z}}_k(i)$ denote the i -th entries in \mathbf{v} and $\bar{\mathbf{z}}_k$, respectively. Then, the newly generated vertices are given by

$$\mathbf{v}_i^{k+1} = \mathbf{o}_k + \mathbf{D}(\mathbf{e}_i)(\bar{\mathbf{z}}_k - \mathbf{o}_k),$$

where \mathbf{e}_i is a unit vector having “1” in the i -th entry. Finally, the new vertex set V_{k+1} can be updated as follows:

$$V_{k+1} = (V_k \setminus \bar{V}_k) \cup V^{k+1}, \quad (13)$$

where V^{k+1} denotes the set of newly generated vertices; e.g., $V^{k+1} = \{\mathbf{v}_1^{k+1}, \mathbf{v}_2^{k+1}\}$ as illustrated in Fig. 2a. Hence, the new polyblock is constructed as $P_{k+1} = \bigcup_{\mathbf{v} \in V_{k+1}} [\mathbf{0}, \mathbf{v}]$.

Algorithm 1 DUE Relays’ Robust EH Scheduling and Beamforming

- 1: Set $\epsilon = 10^{-5}$, initialize vertex set V_k and polyblock P_k
 - 2: Set $r_k^U = 1$ and $r_k^L = 0$ for $k = 0$
 - 3: **while** $|r_k^U - r_k^L| \geq \epsilon$
 - 4: $k \leftarrow k + 1$
 - 5: Update $\mathbf{z}_k = \arg \max_{\mathbf{v} \in V_{k-1}} r(\mathbf{v})$ and $r_k^U = r(\mathbf{z}_k)$
 - 6: **if** $\mathbf{z}_k \in \Omega$ **then**
 - 7: $r_k^L \leftarrow r_k^U$
 - 8: $\mathbf{z}^* \leftarrow \mathbf{z}_k$
 - 9: **else**
 - 10: Find projection $\mathbf{o}_k = s_k \mathbf{z}_k$ via bisection
 - 11: **if** $r(\mathbf{o}_k) \geq r_k^L$
 - 12: $r_k^L \leftarrow r(\mathbf{o}_k)$
 - 13: $\mathbf{z}^* \leftarrow \mathbf{o}_k$
 - 14: **end if**
 - 15: Update vertex set V_k according to (13)
 - 16: Construct new polyblock $P_k = \bigcup_{\mathbf{v} \in V_k} [\mathbf{0}, \mathbf{v}]$
 - 17: **end if**
 - 18: **end while**
 - 19: Retrieve t^* from \mathbf{z}^* and return \mathbf{x}^* by solving (12)
-

The detailed steps of the successive polyblock approximation procedure are shown in Algorithm 1, where $\epsilon > 0$ is the error tolerance that ensures the algorithm returns an ϵ -optimal solution when it terminates. The algorithm can be executed at the source node in a centralized manner. The information required is the matrices \mathbf{A} and \mathbf{B} concerning the relays’ channel conditions and energy status, which can be acquired through information exchange at the beginning of each time slot. For fixed time t , we numerically calculate the maximum SNR $\gamma^*(t)$, and all these points $(t, \gamma^*(t))$ constitute the upper boundary $\partial^+ \Omega$ (denoted by the dashed line in Fig. 2b). Apparently, the upper boundary shows a non-convex feasible set of (t, γ) . Then, we apply Algorithm 1 to search for the global optimum. When the generated polyblocks become closer to the global optimum (denoted by solid lines in Fig. 2b), the gap between the upper and lower throughput bounds will approach the desired accuracy.

IV. NUMERICAL RESULTS

In this section, we assume that each DUE in the D2D network has 3 one-hop neighbors as the relays to enhance the data transmission. The noise at each DUE has zero mean and unit variance. The EH rate \mathbf{c} and the channel \mathbf{h} in the first hop are fixed and known to the DUE relays, while only moment information about the channels \mathbf{g} and \mathbf{z} in the second hop are available to the DUE relays. We first study how the DUE relays’ EH rates and the CUE’s interference requirement affect the throughput performance of the D2D relay network. For simplicity, we assume that all DUE relays have the same EH rate. By varying the CUE’s interference violation probability η , we evaluate the throughput performance with different EH rates. Without loss of generality, we set the channel mean to be $\mathbf{u}_g = \mathbf{u}_z = [1.0, 1.5, 2.0]^T$, and the covariance matrices are symmetric with eigenvalues given by $[2, 2, 2]^T$.

Fig. 3a shows the optimal throughput and EH time for different η and EH rates. It is obvious that the effective throughput increases when we relax the CUE’s probability limit η . In Fig. 3b, we show the DUE relays’ power scaling factors for different EH rates. When the EH rates are small, we observe that all DUE relays transmit at their peak power to fully use the harvested energy. When the EH rates increase, the optimal EH time decreases and the throughput gradually stabilizes at a fixed level as shown in Fig. 3a. This is because the DUE relays have accumulated sufficient energy and the throughput of the D2D network is dominated by the channel conditions as well as the CUE’s interference requirement. Hence, some relays decrease the power scaling factor to suppress the noise at the DRx as shown in Fig. 3b.

In Fig. 4, we examine how the channels \mathbf{g} and \mathbf{z} affect the relays’ power control strategy. In Case 1, we set $\mathbf{h} = [1.0, 2.0, 3.0]^T$ and $\mathbf{u}_g = \mathbf{u}_z = [2, 2, 2]^T$. In Case 2, we update $\mathbf{u}_g = [3, 2, 2]^T$, meaning that the channel in the second hop becomes better. In Case 3, we update $\mathbf{u}_z = [2, 2, 3]^T$, meaning that the interference to the CUE becomes stronger. As a result, we observe performance improvement in Case 2 and degradation in Case 3 as shown in Fig. 4a. The relays’

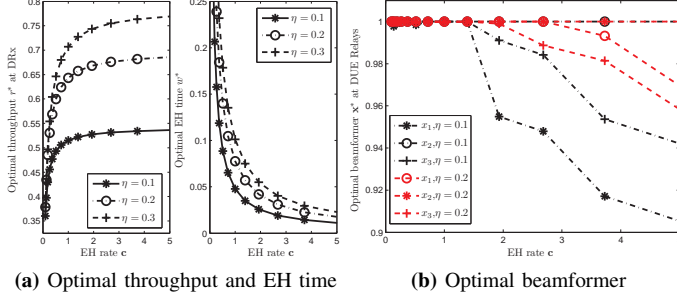


Fig. 3: Performance with EH rates and interference requirements.

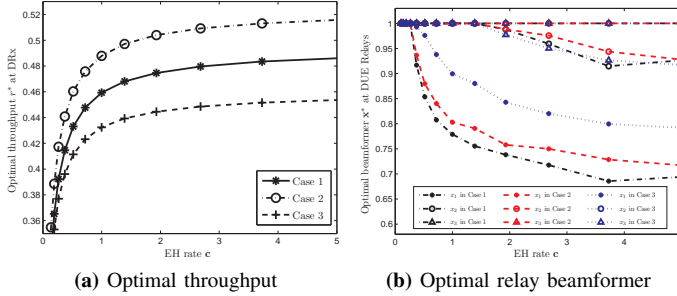


Fig. 4: Performance with EH rates and channel conditions.

optimal power scaling factors in different cases are shown in Fig. 4b. We observe that relay-3 has the best channel in the first hop (i.e., $h_3 \geq h_2 \geq h_1$) in Case 1 and thus it transmits at the peak power (i.e., $x_3 = 1$). In Case 2, the power scaling factor of the DUE relay-1 has been increased due to the improvement of channel g_1 in the second hop. In Case 3, the channel from the DUE relay-3 to the CUE has been improved. Hence, it has to decrease the transmit power to suppress the interference to the CUE.

V. CONCLUSIONS

In this paper, multiple DUE relays are employed to improve the throughput of a D2D network by fully utilizing the harvested energy at different DUE relays. Considering imperfect channel information, we propose a robust formulation for the relays' joint EH scheduling and beamforming problem. Though the performance maximization problem is non-convex, we attain the global optimum by successively approximating its feasible region by regularly-shaped polyblocks.

APPENDIX A PROOF OF PROPOSITION 2

By Definition 3, given $\mathbf{z}^{(1)} \triangleq (t^{(1)}, \gamma^{(1)}) \in \Omega$ and $\mathbf{z}^{(2)} \triangleq (t^{(2)}, \gamma^{(2)}) \preceq \mathbf{z}^{(1)}$, we need to find a solution $\mathbf{x}^{(2)} \in [0, 1]$ such that the probabilistic constraint (5b) is satisfied and $\gamma^{(2)} \leq \bar{\gamma}^{(2)} \triangleq \frac{(\mathbf{x}^{(2)})^T \mathbf{A} \mathbf{x}^{(2)}}{f(t^{(2)}) + (\mathbf{x}^{(2)})^T \mathbf{B} \mathbf{x}^{(2)}}$. Let $\mathbf{x}^{(2)} = \kappa \mathbf{x}^{(1)}$ where κ is a scaling factor. Then, we have

$$\gamma^{(2)} = \frac{(\mathbf{x}^{(2)})^T \mathbf{A} \mathbf{x}^{(2)}}{f(t^{(2)}) + (\mathbf{x}^{(2)})^T \mathbf{B} \mathbf{x}^{(2)}} = \frac{(\mathbf{x}^{(1)})^T \mathbf{A} \mathbf{x}^{(1)}}{\frac{f(t^{(2)})}{\kappa^2} + (\mathbf{x}^{(1)})^T \mathbf{B} \mathbf{x}^{(1)}}. \quad (14)$$

By setting $\kappa^2 = \frac{\gamma^{(2)} f(t^{(2)})}{(\mathbf{x}^{(1)})^T (\mathbf{A} - \gamma^{(2)} \mathbf{B}) \mathbf{x}^{(1)}}$, we can ensure $\gamma^{(2)} \leq \bar{\gamma}^{(2)}$. Moreover, from (14) we have

$$\begin{aligned} \gamma^{(2)} f(t^{(2)}) / \kappa^2 &= (\mathbf{x}^{(1)})^T (\mathbf{A} - \gamma^{(2)} \mathbf{B}) \mathbf{x}^{(1)} \\ &\geq (\mathbf{x}^{(1)})^T (\mathbf{A} - \gamma^{(1)} \mathbf{B}) \mathbf{x}^{(1)} = \gamma^{(1)} f(t^{(1)}), \end{aligned}$$

which implies $\kappa^2 \left(\frac{1}{t^{(2)}} - 2 \right) \leq \frac{\gamma^{(2)}}{\gamma^{(1)}} \left(\frac{1}{t^{(1)}} - 2 \right) \leq \left(\frac{1}{t^{(1)}} - 2 \right)$. Therefore, we have the following inequality:

$$\phi(\mathbf{z}^{(2)}) = \sum_{n=1}^N |z_n|^2 \left(x_n^{(1)} \right)^2 c_n \kappa^2 \left(1/t^{(2)} - 2 \right) \leq \phi(\mathbf{z}^{(1)}).$$

Hence, we can always find $\kappa = \left(\frac{\gamma^{(2)} f(t^{(2)})}{(\mathbf{x}^{(1)})^T (\mathbf{A} - \gamma^{(2)} \mathbf{B}) \mathbf{x}^{(1)}} \right)^{1/2} \leq \left(\frac{1/t^{(1)} - 2}{1/t^{(2)} - 2} \right)^{1/2} \leq 1$ such that $\mathbf{x}^{(2)} = \kappa \mathbf{x}^{(1)}$ and $\mathbb{P}_{\mathbf{z}}(\phi(t^{(2)}, \mathbf{x}^{(2)}) \geq \bar{\phi}) \leq \mathbb{P}_{\mathbf{z}}(\phi(t^{(1)}, \mathbf{x}^{(1)}) \geq \bar{\phi}) \leq \eta$, which implies that $\mathbf{z}^{(2)} \in \Omega$ and thus Ω is normal.

REFERENCES

- [1] A. Asadi, Q. Wang, and V. Mancuso, "A survey on device-to-device communication in cellular networks," *IEEE Commun. Surv. Tut.*, vol. 16, no. 4, pp. 1801–1819, 2014.
- [2] S. Sudevalayam and P. Kulkarni, "Energy harvesting sensor nodes: Survey and implications," *IEEE Commun. Surveys Tuts.*, vol. 13, no. 3, pp. 443–461, Third Quarter 2011.
- [3] A. Nasir, X. Zhou, S. Durrani, and R. Kennedy, "Relaying protocols for wireless energy harvesting and information processing," *IEEE Trans. Wireless Commun.*, vol. 12, no. 7, pp. 3622–3636, Jul. 2013.
- [4] Y. Luo, J. Zhang, and K. B. Letaief, "Relay selection for energy harvesting cooperative communication systems," in *Proc. IEEE GLOBECOM*, Dec. 2013, pp. 2514–2519.
- [5] Y. H. Lee and K. H. Liu, "Battery-aware relay selection for energy-harvesting relays with energy storage," in *Proc. IEEE PIMRC*, Aug. 2015, pp. 1786–1791.
- [6] S. Gong, L. Duan, and N. Gautam, "Optimal scheduling and beamforming in relay networks with energy harvesting constraints," *IEEE Trans. Wireless Commun.*, vol. 15, no. 2, pp. 1226–1238, Feb. 2016.
- [7] M. Fadel, A. El-Keyi, and A. Sultan, "QoS-constrained multiuser peer-to-peer amplify-and-forward relay beamforming," *IEEE Trans. Signal Process.*, vol. 60, no. 3, pp. 1397–1408, Mar. 2012.
- [8] Y. Qin, M. Ding, M. Zhang, H. Yu, and H. Luo, "Relaying robust beamforming for device-to-device communication with channel uncertainty," *IEEE Commun. Lett.*, vol. 18, no. 10, pp. 1859–1862, Oct. 2014.
- [9] M. Hasan, E. Hossain, and D. I. Kim, "Resource allocation under channel uncertainties for relay-aided device-to-device communication underlying LTE-A cellular networks," *IEEE Trans. Wireless Commun.*, vol. 13, no. 4, pp. 2322–2338, Apr. 2014.
- [10] M. N. Tehrani, M. Uysal, and H. Yanikomeroglu, "Device-to-device communication in 5G cellular networks: challenges, solutions, and future directions," *IEEE Commun. Mag.*, vol. 52, no. 5, pp. 86–92, May 2014.
- [11] Q. Li, A. M.-C. So, and W.-K. Ma, "Distributionally robust chance-constrained transmit beamforming for multiuser MISO downlink," in *Proc. IEEE ICASSP*, May. 2014, pp. 3479–3483.
- [12] H. Tuy, "Monotonic optimization: Problems and solution approaches," *SIAM Journal on Optimization*, vol. 11, no. 2, pp. 464–494, Feb. 2000.
- [13] Y. J. A. Zhang, L. Qian, and J. Huang, "Monotonic optimization in communication and networking systems," *Foundations and Trends in Networking*, vol. 7, no. 1, pp. 1–75, 2013.
- [14] J. Gotth and H. Konno, "Maximization of the ratio of two convex quadratic functions over a polytope," *Computational Optimization and Applications*, vol. 20, no. 1, pp. 43–60, 2001.
- [15] S. Zymler, D. Kuhn, and B. Rustem, "Distributionally robust joint chance constraints with second-order moment information," *Math. Program.*, vol. 137, no. 1–2, pp. 167–198, 2013.
- [16] Z.-Q. Luo, W.-K. Ma, A. M.-C. So, Y. Ye, and S. Zhang, "Semidefinite relaxation of quadratic optimization problems," *IEEE Signal Process. Mag.*, vol. 27, no. 3, pp. 20–34, May 2010.